

---

# Wide and Deep Graph Neural Networks with Distributed Online Learning

---

Zhan Gao, Fernando Gama, and Alejandro Ribeiro

Department of Electrical and Systems Engineering  
University of Pennsylvania  
Philadelphia, PA 19104

{gaozhan, fgama, aribeiro}@seas.upenn.edu

## Abstract

Graph neural networks (GNNs) learn representations from network data with naturally distributed architectures. This renders them well-suited candidates for decentralized learning since the operations respect the structure imposed by the underlying graph. Oftentimes, this graph support changes with time, whether it is due to link failures or topology changes caused by mobile components. Modifications to the underlying structure create a mismatch between the graphs on which GNNs were trained and the ones on which they are tested. Online learning can be used to retrain the GNNs at test time, overcoming this issue. However, most online learning algorithms are centralized and work on convex objective functions (which GNNs rarely lead to). This paper puts forth the Wide and Deep GNN (WD-GNN), a novel architecture that can be easily updated with distributed online learning mechanisms. The WD-GNN consists of two components: the wide part is a bank of linear graph filters and the deep part is a convolutional GNN. At training time, the joint architecture learns a relevant nonlinear representation from data. At test time, the deep part is left unchanged, while the wide part is retrained online. Since the wide part is linear, the problem becomes convex, and online optimization algorithms can be used. Furthermore, in order to exploit the distributed nature of the architecture, we propose a distributed online optimization algorithm that updates the wide part at test time, without violating its decentralized nature. We also analyze the stability of the WD-GNN to changes in the underlying topology and derive convergence guarantees for the online retraining procedure. These results indicate the transferability, scalability, and efficiency of the WD-GNN to adapt online to new testing scenarios in a distributed manner. Experiments on the control of robot swarm for flocking corroborate the theory and show the potential of the proposed architecture for distributed online learning.

## 1 Introduction

Graph neural networks (GNNs) [1–6] are nonlinear representation maps that have been shown to perform successfully on graph data in a wide array of tasks involving citation networks [5], recommendation systems [7], source localization [8], power grids [9] and robot swarms [10]. GNNs consist of a cascade of layers, each of which applies a graph convolution (a graph filter) [11], followed by a pointwise nonlinearity [1–6]. One of the key aspects of GNNs is that they are local and distributed. They are local since they require information only from neighboring nodes, and distributed since each node can compute its own output, without need for a centralized unit.

Oftentimes, however, problems of interest exhibit (slight) changes in data structure between training and testing set or involve dynamic systems [12, 13]. For example, in the case of the robot swarm, the

graph is determined by the communication network between robots which is, in turn, determined by their physical proximity. Thus, if robots move, the communication links will change, and the graph support will change as well. Therefore, we oftentimes need to adapt to (slightly) new data structures. GNNs have been shown to be resilient to changes, as proven by the properties of permutation equivariance and stability [14, 15]. While these properties guarantee transference, we can further improve the performance by leveraging online learning approaches.

Online learning is a well-established paradigm that tracks the optimizer of time-varying optimization problems and has been successful as an enabler in the fields of machine learning and signal processing [16]. In a nutshell, online algorithms tackle each modified time instance of the optimization problem, by performing a series of updates on the previously obtained solutions. In order to leverage online learning in GNNs we face two major roadblocks. First, optimality bounds and convergence guarantees are given only for convex problems [17]. Second, online optimization algorithms assume a centralized setting. The latter one is particularly problematic since it violates the local and distributed nature of GNNs, upon which much of its success has been built [10].

This paper puts forward the Wide and Deep Graph Neural Network (WD-GNN) architecture, that is amenable to distributed online learning, while keeping convergence guarantees. We define the WD-GNN as consisting of two components, a deep part which is a nonlinear GNN and a wide part which is a bank of linear graph filters (Section 3). We propose to have an offline phase of training, that need not be distributed, and then an online *retraining* phase, where only the wide part is adapted to the new problem settings. In this way, we learn a nonlinear representation, that can still be adapted online without sacrificing the convex nature of the problem (Section 4). We further develop an algorithm for *distributed* online learning. We prove that the WD-GNN is stable to changes in the underlying graph support, indicating a certain level of robustness to structural changes, and we prove convergence guarantees for the proposed online learning procedure (Section 5). Finally, we perform simulated experiments on robot swarm control (Section 6). Note that proofs, implementation details and another experiment involving movie recommendation systems, can be found in the supplementary material.

## 2 Related work

GNNs have been developed as a nonlinear representation map that is capable of leveraging graph structure present in data. The most popular model for GNNs is the one involving graph convolutions (formally known as graph FIR filters). Several implementations of this model were proposed, including [1] which computes the graph convolution in the spectral domain, [2] which uses a Chebyshev polynomial implementation, [3, 4] which uses a summation polynomial, and [5, 6] which reduce the polynomial to just the first order. All of these are different implementations of the same representation space given by the use of graph convolutional filters to regularize the linear transform of a neural network model. Other popular GNN models include graph attention transforms [18] and CayleyNets [19], see [20] for a general framework.

Online learning has been investigated in designing neural networks (NNs) for dynamically varying problems. Specifically, [21, 22] develop online algorithms for feedforward neural networks with applications in dynamical condition monitoring and aircraft control. More recently, online learning has been used in convolutional neural networks for visual tracking, detection and classification [23, 24]. While these works develop online algorithms for NNs, analysis on the convergence of these algorithms is not presented, except for [25] that proves the convergence of certain online algorithms for radial neural networks only.

## 3 Wide and Deep Graph Neural Networks

Let  $\mathcal{G} = \{\mathcal{V}, \mathcal{E}, \mathcal{W}\}$  describe a *graph*, where  $\mathcal{V} = \{n_1, \dots, n_N\}$  is the set of  $N$  nodes,  $\mathcal{E} \subseteq \mathcal{V} \times \mathcal{V}$  is the set of edges, and  $\mathcal{W} : \mathcal{E} \rightarrow \mathbb{R}$  is the edge weight function. In the case of the robot swarm, each node  $n_i \in \mathcal{V}$  represents a robot, each edge  $(n_j, n_i) \in \mathcal{E}$  represents the communication link between robot  $n_j$  and  $n_i$ , and the weight  $\mathcal{W}(n_j, n_i) = w_{ji} \geq 0$  models the communication channel.

The graph  $\mathcal{G}$  is used to describe the data structure of interest. The data itself is defined on top of the graph and is described by means of a *graph signal*  $\mathbf{X} : \mathcal{V} \rightarrow \mathbb{R}^F$  which assigns an  $F$ -dimensional *feature vector* to each node. For example, in the robot swarm, the signal  $\mathbf{X}(n_i) \in \mathbb{R}^F$  represents the *state* of robot  $n_i$ , typically described by its relative position, velocity or acceleration. The collection

of features across all nodes in the graph can be conveniently denoted with a matrix  $\mathbf{X} \in \mathbb{R}^{N \times F}$  which we call a graph signal as well. Note that each row of  $\mathbf{X}$  corresponds to the feature vector at each node, whereas each column corresponds to the collection of the  $f$ th feature across all nodes.

Describing the data as a graph signal lets us leverage the framework of graph signal processing (GSP) as the mathematical foundation on which to develop algorithms, derive properties and gain insights [11]. In particular, note that  $\mathbf{X}$  is a  $N \times F$  matrix that bares no information about the underlying graph (beyond the fact that it has  $N$  nodes). To be able to relate the graph signal to the specific graph it is supported on, we need a matrix description of the graph. Let  $\mathbf{S} \in \mathbb{R}^{N \times N}$  be a *support matrix* that satisfies  $[\mathbf{S}]_{ij} = 0$  if  $i \neq j$  and  $(n_j, n_i) \notin \mathcal{E}$ . Examples of support matrices commonly used in the literature include the adjacency matrix, the Laplacian matrix, and other normalized versions. The key aspect of the support matrix is that it respects the sparsity of the graph. Thus, when using it as a linear operator on the data  $\mathbf{S}\mathbf{X}$ , we observe that the output at node  $n_i$  for feature  $f$  becomes

$$[\mathbf{S}\mathbf{X}]_{if} = \sum_{j=1}^N [\mathbf{S}]_{ij} [\mathbf{X}]_{jf} = \sum_{j:n_j \in \mathcal{N}_i} [\mathbf{S}]_{ij} [\mathbf{X}]_{jf} \quad (1)$$

where the second equality emphasizes the sparse nature of support, in the sense that only the values of the  $f$ th feature at the neighboring nodes  $n_j \in \mathcal{N}_i$  for  $\mathcal{N}_i = \{n_j \in \mathcal{V} : (n_j, n_i) \in \mathcal{E}\}$  are required to compute the output of the linear operation  $\mathbf{S}\mathbf{X}$  at each node. This renders  $\mathbf{S}\mathbf{X}$  a linear operation that only needs information from neighboring nodes (local) and that can be computed separately at each node (distributed). The operation  $\mathbf{S}\mathbf{X}$  is at the core of GSP since it effectively relates the graph signal with the graph support, and it usually receives the name of a *graph shift* [11].

While, in general, we can think of graph data as given by a pair  $(\mathbf{X}, \mathbf{S})$  consisting of the graph signal  $\mathbf{X}$  and its support  $\mathbf{S}$ , we would like to remark that we only regard  $\mathbf{X}$  as *actionable*. The support  $\mathbf{S}$  is determined by the physical constraints of the problem. For example, in the robot swarm,  $\mathbf{S}$  represents some specific model of communications among robots.

In what follows, we propose the Wide and Deep Graph Neural Network (WD-GNN) architecture. It is a nonlinear map  $\Psi : \mathbb{R}^{N \times F} \rightarrow \mathbb{R}^{N \times G}$  that consists of two components

$$\Psi(\mathbf{X}; \mathbf{S}, \mathcal{A}, \mathcal{B}) = \alpha_D \Phi(\mathbf{X}; \mathbf{S}, \mathcal{A}) + \alpha_W \mathbf{B}(\mathbf{X}; \mathbf{S}, \mathcal{B}) + \beta \quad (2)$$

where  $\Phi(\mathbf{X}; \mathbf{S}, \mathcal{A})$  is called the *deep part* and is a graph neural network (GNN), and  $\mathbf{B}(\mathbf{X}; \mathbf{S}, \mathcal{B})$  is called the *wide part* and is a bank of graph filters. The scalars  $\alpha_D, \alpha_W, \beta$  are preset weights<sup>1</sup>.

### 3.1 Wide component: bank of graph filters

The wide component is a *bank of graph filters* [11]. These are defined as a linear mapping between graph signals  $\mathbf{B} : \mathbb{R}^{N \times F} \rightarrow \mathbb{R}^{N \times G}$ , characterized by a set of weights or *filter taps*  $\mathcal{B} = \{\mathbf{B}_k \in \mathbb{R}^{F \times G}, k = 0, \dots, K\}$  as follows

$$\mathbf{B}(\mathbf{X}; \mathbf{S}, \mathcal{B}) = \sum_{k=0}^K \mathbf{S}^k \mathbf{X} \mathbf{B}_k. \quad (3)$$

The operation to compute the output (3) is often called a *graph convolution* [1, 3].

The output of (3) is another graph signal of dimensions  $N \times G$ . Note that the graph filter has the ability to change the dimension of the feature vector (i.e. from  $F$  to  $G$ ). In fact, to accommodate for the multi-dimensional nature of these features, the graph filter (3) actually acts analogously to the application of a bank of  $FG$  filters, hence the name. Oftentimes, though, we refer to (3) as simply a *graph filter* or a *graph convolution*.

The filtering operation as in (3) is distributed and local, as it can be computed at each node with information relied by neighboring nodes only. To see this, note that the multiplication on the left by  $\mathbf{S}^k$  is the one that mixes information from different nodes (in the columns of  $\mathbf{X}$ ), but since  $\mathbf{S}$  respects the sparsity of the graph and  $\mathbf{S}^k \mathbf{X} = \mathbf{S}(\mathbf{S}^{k-1} \mathbf{X})$  can be seen as repeated applications of  $\mathbf{S}$ , then only the information from neighboring nodes is collected [cf. (1)]. Multiplication on the right by  $\mathbf{B}_k$  actually carries out a linear combination of the entries in the row of  $\mathbf{X}$ , but since these rows

<sup>1</sup>The weights  $\alpha_1, \alpha_2$  and  $\beta$  can also be considered architecture parameters and be trained, if necessary.

consider the individual features of each node, then they do not involve any exchange of information with neighboring nodes. Thus, computing the output of a graph filter (3) is carried out entirely in a distributed manner (each node computes its own output features vector) and involves only local information (there is no need to know the structure nor the information of the entire graph).

In practice, the nodes do not need to know  $\mathbf{S}$  at implementation time. They only need to have communication capabilities so that they can receive the information from neighboring nodes, and computational capabilities to compute a linear combination of the information received from the neighbors. They *do not require* full knowledge of the graph, but only of their immediate neighbors. Thus, in terms of distributed implementation, the graph filtering operation scales seamlessly [15]. We fundamentally use (3) as a mathematical framework that offers a condensed description of the communication exchanges that happen in a network.

### 3.2 Deep component

The deep component is a convolutional *graph neural network* (GNN). These are defined as a nonlinear mapping between graph signals  $\Phi : \mathbb{R}^{N \times F} \rightarrow \mathbb{R}^{N \times G}$ , built as a cascade of graph filters [cf. (3)] and pointwise nonlinearities

$$\Phi(\mathbf{X}; \mathbf{S}, \mathcal{A}) = \mathbf{X}_L \quad \text{with} \quad \mathbf{X}_\ell = \sigma \left( \sum_{k=0}^K \mathbf{S}^k \mathbf{X}_{\ell-1} \mathbf{A}_{\ell k} \right) \quad (4)$$

for  $\ell = 1, \dots, L$ , with  $\sigma : \mathbb{R} \rightarrow \mathbb{R}$  a pointwise nonlinear function, which, in an abuse of notation, denotes its entrywise application in (4); and characterized by the set of filter taps  $\mathcal{A} = \{\mathbf{A}_{\ell k} \in \mathbb{R}^{F_{\ell-1} \times F_\ell}, k = 0, \dots, K, \ell = 1, \dots, L\}$ . The graph signal  $\mathbf{X}_\ell$  at each layer has  $F_\ell$  features, and the input is  $\mathbf{X}_0 = \mathbf{X}$  so that  $F_0 = F$  while the output has  $F_L = G$  features.

There is a vast literature on GNNs. We note that [1–4] all describe the same representation space as (4), they just differ in how the graph convolution (3) is implemented. On the other hand, [5, 6] are restricted to  $K_\ell = 1$  for all  $\ell$ , and thus their representation space is just a subspace of that of (4). Since the results presented here are characterizations of the representation space of (4), they hold for all implementations, and while in the numerical section we implement the graph convolution as a direct polynomial, any of the other implementations could have been used<sup>2</sup>.

## 4 Distributed online learning

We train the WD-GNN (2) by solving the empirical risk minimization (ERM) problem<sup>3</sup> for some cost function  $J : \mathbb{R}^{N \times G} \rightarrow \mathbb{R}$  in a given training set  $\mathcal{T} = \{\mathbf{X}_1, \dots, \mathbf{X}_{|\mathcal{T}|}\}$

$$\min_{\mathcal{A}, \mathcal{B}} \frac{1}{|\mathcal{T}|} \sum_{\mathbf{X} \in \mathcal{T}} J(\Psi(\mathbf{X}; \mathbf{S}, \mathcal{A}, \mathcal{B})). \quad (5)$$

The ERM on a nonlinear neural network model is typically nonconvex, and is usually approximately solved by means of some SGD-based optimization algorithm, exploiting the backpropagation method for efficient computation of the derivatives. Note that the number of parameters in  $\mathcal{A}$  and  $\mathcal{B}$  is determined by the hyperparameters  $L$  (number of layers),  $K_\ell$  (number of filter taps per layer) and  $F_\ell$  (number of features per layer) for the deep part, and  $K$  (number of filter taps) for the wide part. Training is the procedure of applying some SGD-based algorithm for some number of iterations or *training steps* and arriving at some set of parameters  $\mathcal{A}^\dagger$  and  $\mathcal{B}^\dagger$ .

In many problems of interest, the data structures may change (slightly) from the training phase to the testing phase, or we may consider dynamic systems, where the scenario changes naturally with time. The problem of controlling a robot swarm, for instance, exhibits both since the different initializations

<sup>2</sup>We note that no single implementation has consistently outperformed the others in a wide range of diverse problems; this is why we choose to focus on characterizing the representation space, and not in the specifics of implementation.

<sup>3</sup>We took the license to define the ERM problem as in (5) so as to include supervised and unsupervised problems in a single framework. To use (5) for a supervised problem, we just extend  $J$  to operate on an extra input representing the label given in the training set.

of positions and velocities of the swarm lead to different structures at training time and testing time, and since inevitable movements of robots cause the communications links between them to change.

*Online learning* addresses this problem by proposing optimization algorithms that adapt to a continuously changing problem [16]. It operates by adjusting parameters repetitively for each time instance of the problem. Online learning algorithms require convexity of the ERM problem to be able to provide optimality bounds as well as convergence guarantees. However, the ERM problem (5) using the WD-GNN is rarely convex.

To tackle this issue we propose to only *retrain* the *wide* component of the WD-GNN. By considering the deep part fixed  $\mathcal{A} = \mathcal{A}^\dagger$  as obtained from solving (5) over the training set, we can focus on the wide part, which is linear. Thus, we can obtain a new ERM problem, now convex, that can be solved online to find a new set of parameters  $\mathcal{B}$ . In essence, we are leveraging the deep part to learn a *nonlinear representation* from the training set in an offline phase, and then adapt it online to the testing set, but only up to the extent of linear transforms.

Let  $\mathcal{A}^\dagger$  and  $\mathcal{B}^\dagger$  be the parameters learned from the offline phase. At testing time, the implementation scenario may differ from the one that is used for training, leading to a time-varying optimization problem of the form

$$\min_{\mathcal{A}, \mathcal{B}} J_t(\Psi(\mathbf{X}_t; \mathbf{S}_t, \mathcal{A}, \mathcal{B})) \quad (6)$$

where  $J_t(\cdot)$ ,  $\mathbf{X}_t$  and  $\mathbf{S}_t$  are the loss function, the observed signal and the graph structure at time  $t$ , respectively. In the online phase we fix the deep part  $\mathcal{A} = \mathcal{A}^\dagger$ , converting the WD-GNN to a convex model. Then, we retrain the wide part online based on the changing scenario [cf. (32)]. More specifically, we let  $\mathcal{B}_0 = \mathcal{B}^\dagger$  initially and, at time  $t$ , we have parameters  $\mathcal{A}^\dagger$  and  $\mathcal{B}_t$ , input signal  $\mathbf{X}_t$ , output  $\Psi(\mathbf{X}_t; \mathbf{S}_t, \mathcal{A}^\dagger, \mathcal{B}_t)$ , and loss  $J_t(\Psi(\mathbf{X}_t; \mathbf{S}_t, \mathcal{A}^\dagger, \mathcal{B}_t))$ . At time  $t$ , we can then perform a few (probably one) gradient descent step with step size  $\gamma_t$  to update  $\mathcal{B}_t$

$$\mathcal{B}_{t+1} = \mathcal{B}_t - \gamma_t \nabla_{\mathcal{B}} J_t(\Psi(\mathbf{X}_t; \mathbf{S}_t, \mathcal{A}^\dagger, \mathcal{B}_t)). \quad (7)$$

Algorithm 1 in the supplementary material summarizes the above online learning procedure. One major drawback is that this online algorithm is centralized, violating the distributed nature of the WD-GNN. To overcome this issue, we introduce the following method.

#### 4.1 Distributed online algorithm

In decentralized problems, each node  $n_i$  has access to a local loss  $J_{i,t}(\Psi(\mathbf{X}_t; \mathbf{S}_t, \mathcal{A}_i, \mathcal{B}_i))$  with local parameters  $\mathcal{A}_i$  and  $\mathcal{B}_i$ . The goal is to coordinate nodes to minimize the sum-cost  $\sum_{i=1}^N J_{i,t}(\Psi(\mathbf{X}_t; \mathbf{S}_t, \mathcal{A}_i, \mathcal{B}_i))$  while keeping local parameters equal to each other, i.e.,  $\mathcal{A}_i = \mathcal{A}$  and  $\mathcal{B}_i = \mathcal{B}$  for all  $i = 1, \dots, N$ . We can then recast problem (32) as a constrained optimization one

$$\min_{\{\mathcal{B}_i\}_{i=1}^N} \sum_{i=1}^N J_{i,t}(\Psi(\mathbf{X}_t; \mathbf{S}_t, \mathcal{A}^\dagger, \mathcal{B}_i)), \text{ s.t. } \mathcal{B}_i = \mathcal{B}_j \forall i, j : n_j \in \mathcal{N}_i \quad (8)$$

where  $\mathcal{A}_i = \mathcal{A}^\dagger$  for all  $i = 1, \dots, N$  since the deep part is fixed. The constraint  $\mathcal{B}_i = \mathcal{B}_j$  for all  $i, j : n_j \in \mathcal{N}_i$  indicates that  $\mathcal{B}_i = \mathcal{B}$  for all  $i = 1, \dots, N$  under the assumed connectivity of the graph. To solve (8), at time  $t$ , each node  $n_i$  updates its local parameters  $\mathcal{B}_i$  by the recursion

$$\mathcal{B}_{i,t+1} = \frac{1}{|\mathcal{N}_i| + 1} \left( \sum_{j: n_j \in \mathcal{N}_i} \mathcal{B}_{j,t} + \mathcal{B}_{i,t} \right) - \gamma_t \nabla_{\mathcal{B}} J_{i,t}(\Psi(\mathbf{X}_t; \mathbf{S}_t, \mathcal{A}^\dagger, \mathcal{B}_{i,t})) \quad (9)$$

with  $|\mathcal{N}_i|$  the number of neighbors of node  $n_i$ . Put simply, each node  $n_i$  descends its parameters  $\mathcal{B}_{i,t}$  along the local gradient  $\nabla_{\mathcal{B}} J_{i,t}(\Psi(\mathbf{X}_t; \mathbf{S}_t, \mathcal{A}^\dagger, \mathcal{B}_{i,t}))$  and performs the average over the 1-hop neighborhood in the meantime, thus approaching the optimal parameters of (8), while simultaneously driving the local parameters to the consensus.

In a nutshell, the proposed online procedure is of low complexity due to the linearity and guarantees efficient convergence due to the convexity as proved next. Furthermore, it can be implemented in a distributed manner requiring only neighborhood information.

## 5 Stability and convergence

In this section, we establish the stability of the WD-GNN to changes in the underlying graph  $\mathbf{S}$ , that is, we prove that the change in the WD-GNN output caused by the perturbation in  $\mathbf{S}$ , is bounded by the size of perturbation. Then, we prove that the online learning procedure converges to the optimizer set of a time-varying problem, up to an error neighborhood that depends on problem variations.

### 5.1 Stability analysis

The WD-GNN consists of a GNN and a graph filter. Both of these components are permutation equivariant [6, 15] which means that their outputs are unaffected by node reorderings. Since the sum in (2) does not affect this property, WD-GNNs are permutation equivariant as well.

We then consider arbitrary changes to the graph matrix. Let  $\mathbf{S}$  be the given graph and  $\hat{\mathbf{S}}$  a perturbation of it. We measure the size of the perturbation in relative terms as follows. Define the *relative error set*

$$\mathcal{R} = \{\mathbf{E} \in \mathbb{R}^{N \times N} : \mathbf{P}^\top \hat{\mathbf{S}} \mathbf{P} = \mathbf{S} + \mathbf{E} \mathbf{S} + \mathbf{S} \mathbf{E}, \mathbf{E} = \mathbf{E}^\top, \mathbf{P} \in \mathcal{P}\} \quad (10)$$

for  $\mathbf{P}$  in the permutation set  $\mathcal{P} = \{\mathbf{P} \in \{0, 1\}^{N \times N} : \mathbf{P} \mathbf{1} = \mathbf{1}, \mathbf{P}^\top \mathbf{1} = \mathbf{1}\}$ . The relative error set is the set of all symmetric matrices  $\mathbf{E}$  such that, when multiplied with the support matrix  $\mathbf{S}$  and added back, they yield a permutation of the perturbed support  $\hat{\mathbf{S}}$ . Then, we can define *relative perturbation measure* between  $\mathbf{S}$  and  $\hat{\mathbf{S}}$  as

$$d(\mathbf{S}, \hat{\mathbf{S}}) = \min_{\mathbf{E} \in \mathcal{R}} \|\mathbf{E}\|. \quad (11)$$

The relative perturbation measure computes how different is the perturbation  $\hat{\mathbf{S}}$  in terms of the original support  $\mathbf{S}$ , irrespective of the specific ordering of the nodes (given the permutation equivariance property of the WD-GNN). We note that the relative perturbation model ties the size of the perturbation to the topology of the graph through the multiplication of  $\mathbf{E}$  with  $\mathbf{S}$ , thus avoiding the failure to capture structural transformations that typically accompanies the choice of absolute perturbation  $\mathbf{P}^\top \hat{\mathbf{S}} \mathbf{P} = \mathbf{S} + \mathbf{E}$  [15]. The WD-GCNN can be proved stable when built upon integral Lipschitz filters.

**Definition 1** (Integral Lipschitz filters). *Let  $\mathbf{B}(\mathbf{X}; \mathbf{S}, \mathcal{B})$  be a graph filter (3). Denote by  $b_k^{fg} = [\mathbf{B}_k]_{fg}$  and build the graph frequency response  $b^{fg}(\lambda) = \sum_{k=0}^K b_k^{fg} \lambda^k$  satisfying  $|b^{fg}(\lambda)| \leq 1$  [11]. If there exists a constant  $C_L > 0$  such that for all  $\lambda_1, \lambda_2 \in \mathbb{R}$  and for all  $f = 1, \dots, F$  and  $g = 1, \dots, G$ ,*

$$|b^{fg}(\lambda_2) - b^{fg}(\lambda_1)| \leq C_L \frac{|\lambda_2 - \lambda_1|}{|\lambda_1 + \lambda_2|/2}, \quad (12)$$

*we say that the filter  $\mathbf{B}(\mathbf{X}; \mathbf{S}, \mathcal{B})$  is integral Lipschitz.*

Integral Lipschitz filters are those for which the integral of the graph frequency response is Lipschitz continuous. Integral Lipschitz filters satisfy  $|\lambda(b^{fg}(\lambda))'| \leq C_L$  for all  $\lambda$ , for all  $f, g$ , and where  $(b^{fg}(\lambda))' = db^{fg}/d\lambda$ . Such a condition is reminiscent of the scale invariance of wavelet transforms [26]. In any case, examples of integral Lipschitz filters include graph wavelets [27, 28] and can also be enforced by means of penalties during training [29].

We can now establish the stability of the WD-GNN to relative perturbations. Without loss of generality, we assume the single input and single output, i.e.,  $F = G = 1$ , for theoretical analysis.

**Theorem 1.** *Consider the underlying graph  $\mathbf{S} = \mathbf{V} \mathbf{\Lambda} \mathbf{V}^\top$  and the perturbed graph  $\hat{\mathbf{S}}$  with  $N$  nodes. The relative perturbation  $\mathbf{E} = \mathbf{U} \mathbf{\Theta} \mathbf{U}^\top \in \mathcal{R}$  satisfies  $d(\mathbf{S}, \hat{\mathbf{S}}) \leq \|\mathbf{E}\| \leq \epsilon$ . Consider the WD-GNN (2) with integral Lipschitz filters with constant  $C_L$ . Consider also the nonlinearity  $\sigma(\cdot)$  is normalized Lipschitz  $|\sigma(x_1) - \sigma(x_2)| \leq |x_1 - x_2|$  for all  $x_1, x_2 \in \mathbb{R}$  with  $\sigma(0) = 0$ . Then it holds that*

$$\|\Psi(\mathbf{X}; \mathbf{S}, \mathcal{A}, \mathcal{B}) - \Psi(\mathbf{X}; \hat{\mathbf{S}}, \mathcal{A}, \mathcal{B})\| \leq 2C_L(1 + \delta\sqrt{N})(|\alpha_D|L \prod_{\ell=1}^{L-1} F_\ell + |\alpha_W|) \|\mathbf{X}\| \epsilon + \mathcal{O}(\epsilon^2) \quad (13)$$

*where  $\delta = (\|\mathbf{U} - \mathbf{V}\| + 1)^2 - 1$  implies the eigenvector misalignment between  $\mathbf{S}$  and  $\mathbf{E}$ .*

Theorem 1 shows the WD-GNN output is Lipschitz stable to relative graph perturbations up to a stability constant. The constant comprises three terms  $C_L$ ,  $1 + \delta\sqrt{N}$  and  $|\alpha_D|L \prod_{\ell=1}^{L-1} F_\ell + |\alpha_W|$ , indicating effects of the filter property, the graph perturbation and the network architecture, respectively.

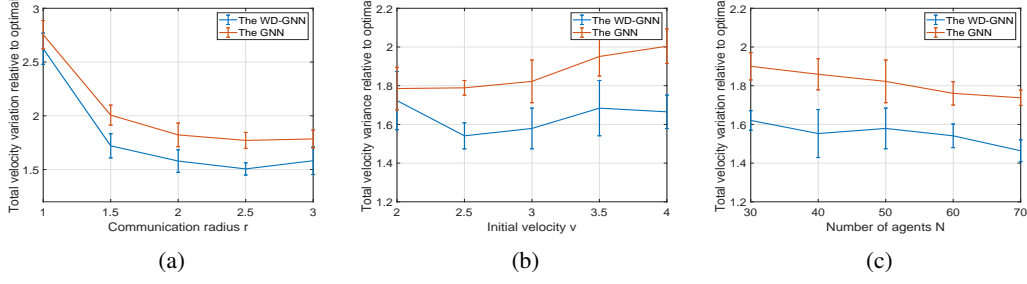


Figure 1. Total velocity variation relative to the optimal controller for the WD-GNN and the GNN. (a) Comparison under different communication radius. (b) Comparison under different initial velocities. (c) Comparison under different numbers of agents.

## 5.2 Convergence analysis

Though the WD-GNN exhibits certain stability to underlying graph changes, the performance degradation is inevitable if this perturbation becomes severe. Furthermore, the graph perturbation is only one example reflecting time-varying scenarios, not to mention changes of the loss function, system observations, etc. Online learning mitigates these effects and adjusts the WD-GNN for changing problems. We show the efficiency of proposed online learning procedure by analyzing its convergence property. Before claiming the main result, we need following standard assumptions.

**Assumption 1.** Consider the time-varying loss function  $J_t(\Psi(\mathbf{X}_t; \mathbf{S}_t, \mathcal{A}, \mathcal{B}))$  with fixed parameters  $\mathcal{A}$ . Let  $\mathcal{B}_t^*$  be an optimal solution of  $J_t(\Psi(\mathbf{X}_t; \mathbf{S}_t, \mathcal{A}, \mathcal{B}))$  at time  $t$ . There exists a sequence  $\{\mathcal{B}_t^*\}_t$  and a constant  $C_B$  such that for all  $t$ , it holds that

$$\|\mathcal{B}_{t+1}^* - \mathcal{B}_t^*\| \leq C_B. \quad (14)$$

**Assumption 2.** Consider the time-varying loss function  $J_t(\Psi(\mathbf{X}_t; \mathbf{S}_t, \mathcal{A}, \mathcal{B}))$  with fixed parameters  $\mathcal{A}$ . When  $\Psi(\mathbf{X}_t; \mathbf{S}_t, \mathcal{A}, \mathcal{B})$  is a linear function of  $\mathcal{B}$ ,  $J_t(\Psi(\mathbf{X}_t; \mathbf{S}_t, \mathcal{A}, \mathcal{B}))$  is differentiable, strongly smooth with constant  $C_{t,s}$  and strongly convex with constant  $C_{t,\ell}$ .

Assumption 1 establishes the correlation between time-varying problems and bounds time variations of changing optimal solutions. Assumption 2 is commonly used in optimization theory and satisfied in practice. Both assumptions are mild, based on which we present the convergence result.

**Theorem 2.** Consider the WD-GNN (2) optimized with the propose online learning algorithm. Let  $J_t(\Psi(\mathbf{X}_t; \mathbf{S}_t, \mathcal{A}, \mathcal{B}))$  be the time-varying loss function satisfying Assumptions 1-2 with constants  $C_B$ ,  $C_{t,s}$  and  $C_{t,\ell}$ . Let also  $\mathcal{B}_t^*$  be the optimal solution of  $J_t(\Psi(\mathbf{X}_t; \mathbf{S}_t, \mathcal{A}, \mathcal{B}))$  and  $\gamma_t = \gamma$  be the step-size of gradient descent. Then, the sequence  $\{\mathcal{B}_t\}_t$  generated by the online learning algorithm in (7) satisfies

$$\|\mathcal{B}_t - \mathcal{B}_t^*\| \leq \left( \prod_{\tau=1}^t m_\tau \right) \|\mathcal{B}_0 - \mathcal{B}_0^*\| + \frac{1 - \hat{m}^t}{1 - \hat{m}} C_B \quad (15)$$

where  $m_t = \max\{|1 - \gamma C_{t,s}|, |1 - \gamma C_{t,\ell}|\}$  is the convergence rate and  $\hat{m} = \max_{1 \leq \tau \leq t} m_\tau$ .

Theorem 2 shows the online learning of the WD-GNN converges to the optimal solution of the time-varying problem up to an limiting error neighborhood. The latter depends on time variations of the optimization problem. If we particularize  $C_B = 0$  with  $m_t = m$  for all  $t$ , we re-obtain the same result for the time-invariant optimization problem, that is the exact convergence of gradient descent.

## 6 Experiments

The goal of the experiment is to learn a decentralized controller that coordinates robots, initially flying at random velocities, to move together at the same velocity while avoiding collisions. Here, we focus on presenting main results. The implementation details, as well as another experiment involving movie recommendation systems, are shown in the supplementary material.

Consider a network of  $N$  robots initially moving at random velocities sampled in the interval  $[-v, v]^2$ . At time  $t$ , each robot  $n_i$  is described by its position  $\mathbf{p}_{i,t} \in \mathbb{R}^2$ , velocity  $\mathbf{v}_{i,t} \in \mathbb{R}^2$  and acceleration

Table 1: Average (std. deviation) of total and final velocity variation.

Architecture/Measurement	Total velocity variation	Final velocity variation
Optimal controller	52( $\pm 2$ )	0.0035( $\pm 0.0001$ )
WD-GNN	84( $\pm 5$ )	0.0119( $\pm 0.0032$ )
WD-GNN (centralized online learning)	79( $\pm 4$ )	0.0065( $\pm 0.0028$ )
WD-GNN (decentralized online learning)	82( $\pm 4$ )	0.0069( $\pm 0.0023$ )
GNN	95( $\pm 6$ )	0.0153( $\pm 0.0030$ )
Graph filter	428( $\pm 105$ )	1.8( $\pm 1.1$ )

$\mathbf{u}_{i,t} \in \mathbb{R}^2$ , the latter being the controllable variable. This problem has an optimal centralized controller  $\mathbf{u}_{i,t}^*$  that can be readily computed [10]. Such a solution requires knowledge of the positions and velocities of all robots and thus demands a centralized computation unit. In the decentralized setting, we assume robot  $n_i$  can only communicate with robot  $n_j$  if they are within the communication radius  $r$ , i.e.,  $\|\mathbf{p}_{i,t} - \mathbf{p}_{j,t}\| \leq r$ . We establish the communication graph  $\mathcal{G}_t$  with the node set  $\mathcal{V}$  for robots and the edge set  $\mathcal{E}_t$  for available communication links, and the graph matrix  $\mathbf{S}_t$  is the associated adjacency matrix.

We use imitation learning [30] to train the WD-GNN for a decentralized controller on accelerations  $\mathbf{U}_t = [\mathbf{u}_{1,t}, \dots, \mathbf{u}_{N,t}]^T = \Psi(\mathbf{X}_t; \mathbf{S}_t, \mathcal{A}, \mathcal{B}) \in \mathbb{R}^{N \times 2}$ , where  $\mathbf{X}_t$  is the graph signal that collects positions and velocities of neighbors at each robot [10]. At testing time, we measure the variation in velocity among the robots over the whole trajectory and also at the final time instant [10]. In a way, the total velocity variation includes how long it takes for the team to be coordinated, while the final velocity variation tells how well the task was finally accomplished.

We first compare the optimal controller, the GNN and the graph filter with the WD-GNN without retraining in the initial condition  $r = 2m$ ,  $v = 3m/s$  and  $N = 50$  (Table 1). We see that the WD-GNN exhibits the best performance in both performance measures. We attribute this behavior to the increased representation power of the WD-GNN as a combined architecture. The GNN takes the second place, while the graph filter performs much worse than the other two architectures. This is because the optimal distributed controller is known to be nonlinear [31].

To account for the adaptability to different initial conditions of the proposed model in comparison with the GNN, we run simulations for changing communication radius (Fig. 1a), changing initial velocities  $v$  (Fig. 1b) and changing numbers of agents  $N$  (Fig. 1c). These experiments show an improved robustness of the WD-GNN. We display results as the relative change in the total velocity variation to the optimal controller. Fig. 1a shows that the performance increases as the communication radius  $r$  increases, which is expected since the robots now have access to farther information. In Fig. 1b, we observe the flocking problem becomes harder with the increase of initial velocity  $v$ , since it is reasonably harder to control robots that move very fast in random directions. As for the number of agents  $N$ , the relative total velocity variation decreases when the number of agents  $N$  increases, which is explained by the fact that the optimization problem becomes easier to solve with increased node exchanges in larger graphs.

Finally, we test the improvement on the WD-GNN with online learning. We consider the centralized online optimization algorithm as the baseline, with the velocity variation as the instantaneous loss function in (32). We test the proposed distributed optimization algorithm (9), where the instantaneous loss function is the velocity variance of neighboring robots. Results are shown in Table 1. We see the total and final velocity variation get reduced for both centralized and decentralized online algorithms, indicating that the WD-GNN is successfully adapting to the changing communication network. The improvement in final velocity variation is more noticeable, since the effects of single time-updates get compounded.

## 7 Conclusion

We propose the Wide and Deep Graph Neural Network architecture and consider a distributed online learning scenario. The proposed architecture consists of a bank of filters (wide part) and a GNN (deep part), leading to a local and distributed architecture, that we proved is stable to small changes in the underlying graph support. To address more general time-varying scenarios without compromising the distributed nature of the architecture, we proposed a distributed online learning

optimization. By fixing the deep part, and retraining online only the wide part, we manage to obtain a convex optimization problem, and thus proved convergence guarantees of online learning algorithms. Numerical experiments are performed on learning decentralized controllers for flocking a robot swarm, showing the success of WD-GNNs in adapting to time-varying scenarios. Future research involves the online retraining of the deep part, as well as obtaining convergence guarantees for the distributed online learning algorithm.

## Broad Impacts

Graph neural networks are nonlinear representation maps that are computationally inexpensive and descriptive enough to capture a wide range of behaviors. They are also local and distributed, which makes them ideal for deployment over physical networks. In the particular case of dynamic multi-agent systems, the issue arises in that the graph support changes with time, requiring for GNNs to be able to adapt to unseen scenarios in an online manner. In this paper, we have developed one such model that can learn online, and most importantly, do so without violating the decentralized nature of the architecture. The current limitations of the proposed method are that only the linear part is being adapted online, and that there are still no convergence guarantees for the distributed online algorithm (only for the centralized online algorithm). In any case, online distributed learning is a key aspect in many real-world application, such as search and rescue, map exploration, and path planning; applications of which flocking is a proof-of-concept that can lay the groundwork for more involved scenarios.

## Acknowledgments

Supported by NSF CCF 1717120, ARO W911NF1710438, ARL DCIST CRA W911NF-17-2-0181, ISTC-WAS and Intel DevCloud.

## References

- [1] J. Bruna, W. Zaremba, A. Szlam, and Y. LeCun, "Spectral networks and deep locally connected networks on graphs," in *2nd Int. Conf. Learning Representations*. Banff, AB: Assoc. Comput. Linguistics, 14-16 Apr. 2014, pp. 1–14.
- [2] M. Defferrard, X. Bresson, and P. Vandergheynst, "Convolutional neural networks on graphs with fast localized spectral filtering," in *30th Conf. Neural Inform. Process. Syst.* Barcelona, Spain: Neural Inform. Process. Foundation, 5-10 Dec. 2016, pp. 3844–3858.
- [3] F. Gama, A. G. Marques, G. Leus, and A. Ribeiro, "Convolutional neural network architectures for signals supported on graphs," *IEEE Trans. Signal Process.*, vol. 67, no. 4, pp. 1034–1049, Feb. 2019.
- [4] F. Wu, A. Souza, T. Zhang, C. Fifty, T. Yu, and K. Weinberger, "Simplifying graph convolutional networks," in *36th Int. Conf. Mach. Learning*, vol. 97. Long Beach, CA: Proc. Mach. Learning Res., 9-15 June 2019, pp. 6861–6871.
- [5] T. N. Kipf and M. Welling, "Semi-supervised classification with graph convolutional networks," in *5th Int. Conf. Learning Representations*. Toulon, France: Assoc. Comput. Linguistics, 24-26 Apr. 2017, pp. 1–14.
- [6] K. Xu, W. Hu, J. Leskovec, and S. Jegelka, "How powerful are graph neural networks?" in *7th Int. Conf. Learning Representations*. New Orleans, LA: Assoc. Comput. Linguistics, 6-9 May 2019, pp. 1–17.
- [7] R. Ying, R. He, K. Chen, P. Eksombatchai, W. L. Hamilton, and J. Leskovec, "Graph convolutional neural networks for web-scale recommender systems," in *International Conference on Knowledge Discovery*, 2018.
- [8] Z. Gao, E. Isufi, and A. Ribeiro, "Stochastic graph neural networks," in *45th IEEE Int. Conf. Acoust., Speech and Signal Process.* Barcelona, Spain: IEEE, 4-8 May 2020.
- [9] D. Owerko, F. Gama, and A. Ribeiro, "Optimal power flow using graph neural networks," in *45th IEEE Int. Conf. Acoust., Speech and Signal Process.* Barcelona, Spain: IEEE, 4-8 May 2020.

- [10] E. Tolstaya, F. Gama, J. Paulos, G. Pappas, V. Kumar, and A. Ribeiro, “Learning decentralized controllers for robot swarms with graph neural networks,” in *Conf. Robot Learning 2019*. Osaka, Japan: Int. Found. Robotics Res., 30 Oct.-1 Nov. 2019.
- [11] A. Ortega, P. Frossard, J. Kovačević, J. M. F. Moura, and P. Vandergheynst, “Graph signal processing: Overview, challenges and applications,” *Proc. IEEE*, vol. 106, no. 5, pp. 808–828, May 2018.
- [12] G. Frahling, P. Indyk, and C. Sohler, “Sampling in dynamic data streams and applications,” *International Journal of Computational Geometry & Applications*, vol. 18, no. 01n02, pp. 3–28, 2008.
- [13] M. K. Helwa and A. P. Schoellig, “Multi-robot transfer learning: A dynamical system perspective,” in *2017 IEEE/RSJ International Conference on Intelligent Robots and Systems (IROS)*, 2017, pp. 4702–4708.
- [14] D. Zou and G. Lerman, “Graph convolutional neural networks via scattering,” *Appl. Comput. Harmonic Anal.*, 13 June 2019, accepted for publication (in press). [Online]. Available: <http://doi.org/10.1016/j.acha.2019.06.003>
- [15] F. Gama, J. Bruna, and A. Ribeiro, “Stability properties of graph neural networks,” *arXiv:1905.04497v3 [cs.LG]*, 22 Apr. 2020. [Online]. Available: <http://arxiv.org/abs/1905.04497>
- [16] N. Dabbagh and B. Bannan-Ritland, *Online learning: Concepts, strategies, and application*. Pearson/Merrill/Prentice Hall Upper Saddle River, NJ, 2005.
- [17] S. Shalev-Shwartz, “Online learning and online convex optimization,” *Foundations and Trends® in Machine Learning*, vol. 4, no. 2, pp. 107–194, 2012.
- [18] P. Veličković, G. Cucurull, A. Casanova, A. Romero, P. Liò, and Y. Bengio, “Graph attention networks,” in *6th Int. Conf. Learning Representations*. Vancouver, BC: Assoc. Comput. Linguistics, 30 Apr.-3 May 2018, pp. 1–12.
- [19] R. Levie, F. Monti, X. Bresson, and M. M. Bronstein, “CayleyNets: Graph convolutional neural networks with complex rational spectral filters,” *IEEE Trans. Signal Process.*, vol. 67, no. 1, pp. 97–109, Jan. 2019.
- [20] E. Isufi, F. Gama, and A. Ribeiro, “EdgeNets: Edge varying graph neural networks,” *arXiv:2001.07620v2 [cs.LG]*, 12 March 2020. [Online]. Available: <http://arxiv.org/abs/2001.07620>
- [21] J. Sanz, R. Perera, and C. Huerta, “Gear dynamics monitoring using discrete wavelet transformation and multi-layer perceptron neural networks,” *Applied Soft Computing*, vol. 12, no. 9, pp. 2867–2878, 2012.
- [22] Y. Li, N. Sundararajan, P. Saratchandran, and Z. Wang, “Robust neuro- $h_\infty$  controller design for aircraft auto-landing,” *IEEE Transactions on Aerospace and Electronic Systems*, vol. 40, no. 1, pp. 158–167, 2004.
- [23] S. Hong, T. You, S. Kwak, and B. Han, “Online tracking by learning discriminative saliency map with convolutional neural network,” in *International Conference on Machine Learning*, 2015.
- [24] P. Molchanov, X. Yang, S. Gupta, K. Kim, S. Tyree, and J. Kautz, “Online detection and classification of dynamic hand gestures with recurrent 3d convolutional neural networks,” in *Conference on Computer Vision and Pattern Recognition*, 2016.
- [25] K. J. Ho, C. S. Leung, and J. Sum, “Convergence and objective functions of some fault/noise-injection-based online learning algorithms for rbf networks,” *IEEE Transactions on Neural Networks*, vol. 21, no. 6, pp. 938–947, 2010.
- [26] I. Daubechies, *Ten Lectures on Wavelets*, ser. CBMS-NSF Regional Conf. Series Appl. Math. Philadelphia, PA: SIAM, 1992, vol. 61.
- [27] D. K. Hammond, P. Vandergheynst, and R. Gribonval, “Wavelets on graphs via spectral graph theory,” *Appl. Comput. Harmonic Anal.*, vol. 30, no. 2, pp. 129–150, March 2011.
- [28] D. I. Shuman, C. Wiesmeyr, N. Holighaus, and P. Vandergheynst, “Spectrum-adapted tight graph wavelet and vertex-frequency frames,” *IEEE Trans. Signal Process.*, vol. 63, no. 16, pp. 4223–4235, Aug. 2015.

- [29] F. Gama, J. Bruna, and A. Ribeiro, “Stability of graph neural networks to relative perturbations,” in *45th IEEE Int. Conf. Acoust., Speech and Signal Process.* Barcelona, Spain: IEEE, 4-8 May 2020.
- [30] S. Ross and J. A. Bagnell, “Efficient reductions for imitation learning,” in *13th Int. Conf. Artificial Intell., Statist.* Sardinia, Italy: Proc. Mach. Learning Res., 13-15 May 2010, pp. 661–668.
- [31] H. S. Witsenhausen, “A counterexample in stochastic optimum control,” *SIAM J. Control*, vol. 6, no. 1, pp. 131–147, 1968.
- [32] A. Simonetto, “Time-varying convex optimization via time-varying averaged operators,” *arXiv:1704.07338v3 [math.OC]*, 24 Apr. 2017. [Online]. Available: <https://arxiv.org/abs/1704.07338>
- [33] W. Huang, A. G. Marques, and A. Ribeiro, “Rating prediction via graph signal processing,” *IEEE Trans. Signal Process.*, vol. 66, no. 19, pp. 5066–5081, 2018.
- [34] M. F. Harper and J. A. Konstan, “The movielens datasets: History and context,” *ACM Trans. Interact. Intell. Syst.*, vol. 5, no. 4, pp. 19:(1–19), 2016.

# Supplementary Materials for ‘Wide and Deep Graph Neural Networks with Distributed Online Learning’

## A Proofs

### A.1 Proof of Theorem 1

We need the following lemma in the proof.

**Lemma 1.** Consider the underlying graph  $\mathbf{S} = \mathbf{V}\mathbf{\Lambda}\mathbf{V}^\top$  and the perturbed graph  $\hat{\mathbf{S}}$  with  $N$  nodes. The relative perturbation  $\mathbf{E} = \mathbf{U}\mathbf{\Theta}\mathbf{U}^\top \in \mathcal{R}$  satisfies  $d(\mathbf{S}, \hat{\mathbf{S}}) \leq \|\mathbf{E}\| \leq \epsilon$ . Consider the integral Lipschitz filter [cf. Definition 1 in full paper] with  $F = 1$  input feature,  $G = 1$  output feature and integral Lipschitz constant  $C_L$ . Then, the output difference between filters  $\mathbf{B}(\mathbf{X}; \mathbf{S}, \mathcal{B})$  and  $\mathbf{B}(\mathbf{X}; \hat{\mathbf{S}}, \mathcal{B})$  satisfies

$$\|\mathbf{B}(\mathbf{X}; \mathbf{S}, \mathcal{B}) - \mathbf{B}(\mathbf{X}; \hat{\mathbf{S}}, \mathcal{B})\| \leq 2C_L(1 + \sigma\sqrt{N})\|\mathbf{X}\|\epsilon + \mathcal{O}(\epsilon^2) \quad (16)$$

where  $\delta = (\|\mathbf{U} - \mathbf{V}\| + 1)^2 - 1$  implies the eigenvector misalignment between  $\mathbf{S}$  and  $\mathbf{E}$ .

*Proof.* With  $F = 1$  input feature  $\mathbf{X} \in \mathbb{R}^{N \times 1}$  and  $G = 1$  output feature  $\mathbf{B}(\mathbf{X}; \mathbf{S}, \mathcal{B}), \mathbf{B}(\mathbf{X}; \hat{\mathbf{S}}, \mathcal{B}) \in \mathbb{R}^{N \times 1}$ , the output difference can be represented by

$$\|\mathbf{B}(\mathbf{X}; \mathbf{S}, \mathcal{B}) - \mathbf{B}(\mathbf{X}; \hat{\mathbf{S}}, \mathcal{B})\| = \left\| \sum_{k=0}^K b_k^{11} \mathbf{S}^k \mathbf{X} - \sum_{k=0}^K b_k^{11} \hat{\mathbf{S}}^k \mathbf{X} \right\| \quad (17)$$

with filter parameters  $\mathcal{B} = \{b_0^{11}, \dots, b_K^{11}\}$ . We then refer to Theorem 3 in [15] to complete the proof.  $\square$

*Proof of Theorem 1.* The output difference between  $\Psi(\mathbf{X}; \mathbf{S}, \mathcal{A}, \mathcal{B})$  and  $\Psi(\mathbf{X}; \hat{\mathbf{S}}, \mathcal{A}, \mathcal{B})$  can be divided into the wide part difference and the deep part difference

$$\|\Psi(\mathbf{X}; \mathbf{S}, \mathcal{A}, \mathcal{B}) - \Psi(\mathbf{X}; \hat{\mathbf{S}}, \mathcal{A}, \mathcal{B})\| \leq \|\Phi(\mathbf{X}; \mathbf{S}, \mathcal{A}) - \Phi(\mathbf{X}; \hat{\mathbf{S}}, \mathcal{A})\| + \|\mathbf{B}(\mathbf{X}; \mathbf{S}, \mathcal{B}) - \mathbf{B}(\mathbf{X}; \hat{\mathbf{S}}, \mathcal{B})\| \quad (18)$$

where the triangle inequality is used. Let us consider these two terms separately.

**The wide term.** By using Lemma 1, we bound the wide part difference as

$$\|\mathbf{B}(\mathbf{X}; \mathbf{S}, \mathcal{B}) - \mathbf{B}(\mathbf{X}; \hat{\mathbf{S}}, \mathcal{B})\| \leq 2C_L(1 + \sigma\sqrt{N})\epsilon + \mathcal{O}(\epsilon^2) \quad (19)$$

**The deep term.** At layer  $\ell$ , the graph convolution can be considered as the application of  $F_{\ell-1}F_\ell$  filters, i.e.,

$$\left[ \sum_{k=0}^K \mathbf{S}^k \mathbf{X}_{\ell-1} \mathbf{A}_{\ell k} \right]_f = \sum_{g=1}^{F_{\ell-1}} \sum_{k=0}^K a_{\ell k}^{fg} \mathbf{S}^k [\mathbf{X}_{\ell-1}]_g \quad (20)$$

for  $f = 1, \dots, F_\ell$ , where  $a_{\ell k}^{fg} = [\mathbf{A}_{\ell k}]_{fg}$  is the  $(f, g)$ th entry of matrix  $\mathbf{A}_{\ell k}$  and  $[\cdot]_f$  represents the  $f$ th column. We denote by  $\mathbf{G}_\ell^{fg}(\mathbf{S})[\mathbf{X}_{\ell-1}]_g = \sum_{k=0}^K a_{\ell k}^{fg} \mathbf{S}^k [\mathbf{X}_{\ell-1}]_g$  and  $\mathbf{x}_{\ell-1}^g = [\mathbf{X}_{\ell-1}]_g$  for convenience of following derivation. By using (20) and substituting the GNN architecture [(4) in full paper] into the deep part difference, we get

$$\begin{aligned} \|\Phi(\mathbf{X}; \mathbf{S}, \mathcal{A}) - \Phi(\mathbf{X}; \hat{\mathbf{S}}, \mathcal{A})\| &= \left\| \sigma \left( \sum_{f=1}^{F_{L-1}} \mathbf{G}_L^{1f}(\mathbf{S}) \mathbf{x}_{L-1}^f \right) - \sigma \left( \sum_{f=1}^{F_{L-1}} \mathbf{G}_L^{1f}(\hat{\mathbf{S}}) \hat{\mathbf{x}}_{L-1}^f \right) \right\| \\ &\leq \sum_{f=1}^{F_{L-1}} \left\| \mathbf{G}_L^{1f}(\mathbf{S}) \mathbf{x}_{L-1}^f - \mathbf{G}_L^{1f}(\hat{\mathbf{S}}) \hat{\mathbf{x}}_{L-1}^f \right\| \end{aligned} \quad (21)$$

where the second inequality is because the nonlinearity  $\sigma$  is normalized Lipschitz and the triangle inequality. By adding and subtracting  $\mathbf{G}_L^{1f}(\hat{\mathbf{S}}) \mathbf{x}_{L-1}^f$  into the terms in the norm, we have

$$\begin{aligned} \left\| \mathbf{G}_L^{1f}(\mathbf{S}) \mathbf{x}_{L-1}^f - \mathbf{G}_L^{1f}(\hat{\mathbf{S}}) \hat{\mathbf{x}}_{L-1}^f \right\| &\leq \left\| \mathbf{G}_L^{1f}(\mathbf{S}) \mathbf{x}_{L-1}^f - \mathbf{G}_L^{1f}(\hat{\mathbf{S}}) \mathbf{x}_{L-1}^f \right\| + \left\| \mathbf{G}_L^{1f}(\hat{\mathbf{S}}) \mathbf{x}_{L-1}^f - \mathbf{G}_L^{1f}(\hat{\mathbf{S}}) \hat{\mathbf{x}}_{L-1}^f \right\| \\ &\leq \left\| \mathbf{G}_L^{1f}(\mathbf{S}) \mathbf{x}_{L-1}^f - \mathbf{G}_L^{1f}(\hat{\mathbf{S}}) \mathbf{x}_{L-1}^f \right\| + \left\| \mathbf{G}_L^{1f}(\hat{\mathbf{S}}) \right\| \left\| \mathbf{x}_{L-1}^f - \hat{\mathbf{x}}_{L-1}^f \right\| \end{aligned} \quad (22)$$

For the first term in (22), by using Lemma 1, we get

$$\|\mathbf{G}_L^{1f}(\mathbf{S})\mathbf{x}_{L-1}^f - \mathbf{G}_L^{1f}(\hat{\mathbf{S}})\mathbf{x}_{L-1}^f\| \leq 2C_L(1 + \sigma\sqrt{N})\|\mathbf{x}_{L-1}^f\|\epsilon + \mathcal{O}(\epsilon^2). \quad (23)$$

In terms of the term  $\|\mathbf{x}_{L-1}^f\|$ , we observe that

$$\|\mathbf{x}_{L-1}^f\| = \left\| \sigma \left( \sum_{g=1}^{F_{L-2}} \mathbf{G}_{L-1}^{fg}(\mathbf{S})\mathbf{x}_{L-2}^g \right) \right\| \leq \sum_{g=1}^{F_{L-2}} \|\mathbf{G}_{L-1}^{fg}(\mathbf{S})\mathbf{x}_{L-2}^g\| \leq \sum_{g=1}^{F_{L-2}} \|\mathbf{x}_{L-2}^g\| \quad (24)$$

where we use the triangle inequality, followed by the bound on filters [11], i.e., the filter frequency response  $|a_{L-1}^{fg}(\lambda)| = \left| \sum_{k=0}^K a_{(L-1)k}^{fg} \lambda^k \right| \leq 1$ . We follow this recursion to obtain

$$\|\mathbf{x}_{L-1}^f\| \leq \prod_{\ell=1}^{L-2} F_\ell \|\mathbf{x}_0^1\| \quad (25)$$

where  $\|\mathbf{x}_0^1\| = \|\mathbf{X}\|$  by definition since the number of input feature  $F_0 = F = 1$ . By substituting (25) into (23), we have

$$\|\mathbf{G}_L^{1f}(\mathbf{S})\mathbf{x}_{L-1}^f - \mathbf{G}_L^{1f}(\hat{\mathbf{S}})\mathbf{x}_{L-1}^f\| \leq 2C_L(1 + \sigma\sqrt{N}) \prod_{\ell=1}^{L-2} F_\ell \|\mathbf{X}\| \epsilon + \mathcal{O}(\epsilon^2) \quad (26)$$

For the second term in (22), by again using the filter bound [11], we get

$$\|\mathbf{G}_L^{1f}(\hat{\mathbf{S}})\|\|\mathbf{x}_{L-1}^f - \hat{\mathbf{x}}_{L-1}^f\| \leq \|\mathbf{x}_{L-1}^f - \hat{\mathbf{x}}_{L-1}^f\|. \quad (27)$$

By substituting (26) and (27) into (22) and the latter into (21), we have

$$\|\Phi(\mathbf{X}; \mathbf{S}, \mathcal{A}) - \Phi(\mathbf{X}; \hat{\mathbf{S}}, \mathcal{A})\| \leq \sum_{f=1}^{F_{L-1}} \|\mathbf{x}_{L-1}^f - \hat{\mathbf{x}}_{L-1}^f\| + 2C_L(1 + \sigma\sqrt{N}) \prod_{\ell=1}^{L-1} F_\ell \|\mathbf{X}\| \epsilon + \mathcal{O}^2(\epsilon). \quad (28)$$

From (28), we observe that the output difference of  $L$ th layer depends on that of  $(L-1)$ th layer. Repeating this recursion until the input layer, we have

$$\|\Phi(\mathbf{X}; \mathbf{S}, \mathcal{A}) - \Phi(\mathbf{X}; \hat{\mathbf{S}}, \mathcal{A})\| \leq 2C_L(1 + \sigma\sqrt{N})^L \prod_{\ell=1}^{L-1} F_\ell \|\mathbf{X}\| \epsilon + \mathcal{O}^2(\epsilon) \quad (29)$$

where we use the initial condition that  $\|\mathbf{x}_0^1 - \hat{\mathbf{x}}_0^1\| = \|\mathbf{X} - \mathbf{X}\| = 0$ .

Together, by substituting (19) and (29) into (18), we complete the proof

$$\|\Psi(\mathbf{X}; \mathbf{S}, \mathcal{A}, \mathcal{B}) - \Psi(\mathbf{X}; \hat{\mathbf{S}}, \mathcal{A}, \mathcal{B})\| \leq 2C_L(1 + \sigma\sqrt{N}) \left( |\alpha_W| + |\alpha_D| L \prod_{\ell=1}^{L-1} F_\ell \right) \|\mathbf{X}\| \epsilon + \mathcal{O}^2(\epsilon). \quad (30)$$

□

## A.2 Proof of Theorem 2

*Proof.* Let  $\mathcal{A}^\dagger$  and  $\mathcal{B}^\dagger$  be the learned parameters from the offline phase. The proposed online learning fixes the deep part, i.e., it freezes the parameters  $\mathcal{A} = \mathcal{A}^\dagger$ , and retrain the wide part online. The model  $\Psi(\mathbf{X}; \mathbf{S}, \mathcal{A}, \mathcal{B})$  can then be represented as a function of  $\mathcal{B}$  while considering  $\mathcal{A} = \mathcal{A}^\dagger$  as constant

$$\Psi(\mathbf{X}; \mathbf{S}, \mathcal{A}^\dagger, \mathcal{B}) = \alpha_D \Phi(\mathbf{X}; \mathbf{S}, \mathcal{A}^\dagger) + \alpha_W \mathbf{B}(\mathbf{X}; \mathbf{S}, \mathcal{B}) + \beta = \hat{\Psi}(\mathbf{X}; \mathbf{S}, \mathcal{B}). \quad (31)$$

Given the graph signal  $\mathbf{X}$  and the graph matrix  $\mathbf{S}$ ,  $\hat{\Psi}(\mathbf{X}; \mathbf{S}, \mathcal{B})$  is a linear function of  $\mathcal{B}$  since both the graph filter  $\mathbf{B}(\mathbf{X}; \mathbf{S}, \mathcal{B})$  and the combination way of two components are linear.

At testing time  $t$ , the sampled optimization problem [(6) in full paper] is translated to

$$\min_{\mathcal{B}} J_t(\hat{\Psi}(\mathbf{X}_t; \mathbf{S}_t, \mathcal{B})) \quad (32)$$

where  $J_t(\cdot)$ ,  $\mathbf{X}_t$  and  $\mathbf{S}_t$  are given instantaneous loss function, observed signal and graph matrix at time  $t$ . Since  $\hat{\Psi}(\mathbf{X}_t; \mathbf{S}_t, \mathcal{B})$  is a linear function of  $\mathcal{B}$ ,  $J_t(\hat{\Psi}(\mathbf{X}_t; \mathbf{S}_t, \mathcal{B}))$  is differentiable, strongly smooth with constant  $C_{t,s}$  and strongly convex with constant  $C_{t,\ell}$  based on Assumption 2. We then refer to Corollary 7.1 in [32] to complete the proof.

□

## B Implementation details for robot swarm flocking

We consider a network with  $N$  robots initially moving at random velocities. At time  $t$ , each robot  $n_i$  is described by its position  $\mathbf{p}_{i,t} \in \mathbb{R}^2$ , velocity  $\mathbf{v}_{i,t} \in \mathbb{R}^2$ , and controls its acceleration  $\mathbf{u}_{i,t} \in \mathbb{R}^2$  for the next state

$$\mathbf{p}_{i,t+1} = \mathbf{p}_{i,t} + \mathbf{v}_{i,t}T_s + \frac{1}{2}\mathbf{u}_{i,t}T_s^2, \quad \mathbf{v}_{i,t+1} = \mathbf{v}_{i,t} + \mathbf{u}_{i,t}T_s \quad (33)$$

where  $T_s$  is the sampling time and  $\mathbf{u}_{i,t}$  is held constant during the sampling time interval  $[T_s t, T_s(t+1)]$ . Our purpose is to control accelerations  $\mathbf{U}_t = [\mathbf{u}_{1,t}, \dots, \mathbf{u}_{N,t}]^\top \in \mathbb{R}^{N \times 2}$  such that robots will move at the same velocity without collision. There is an optimal solution for accelerations [31]

$$\mathbf{u}_{i,t}^* = - \sum_{j=1}^N (\mathbf{v}_{i,t} - \mathbf{v}_{j,t}) - \sum_{j=1}^N \nabla_{\mathbf{p}_{i,t}} V(\mathbf{p}_{i,t}, \mathbf{p}_{j,t}), \quad \forall i = 1, \dots, N \quad (34)$$

with

$$V(\mathbf{p}_{i,t}, \mathbf{p}_{j,t}) = \begin{cases} \frac{1}{\|\mathbf{p}_{i,t} - \mathbf{p}_{j,t}\|^2} - \log(\|\mathbf{p}_{i,t} - \mathbf{p}_{j,t}\|^2), & \text{if } \|\mathbf{p}_{i,t} - \mathbf{p}_{j,t}\| \leq \rho \\ \frac{1}{\rho^2} - \log(\rho^2), & \text{otherwise} \end{cases} \quad (35)$$

the collision avoidance potential. The computation of  $\mathbf{u}_{i,t}^*$  requires instantaneous positions and velocities of all robots over network. As such, it is centralized that cannot be implemented in practice where each robot only has access to local neighborhood information.

In the decentralized setting, robot  $n_i$  can communicate with robot  $n_j$  if and only if they are within the communication radius  $r$ , i.e., there is a communication link  $(n_i, n_j)$  if  $\|\mathbf{p}_{i,t} - \mathbf{p}_{j,t}\| \leq r$ . We establish the communication graph  $\mathcal{G}_t$  with the node set  $\mathcal{V} = \{n_1, \dots, n_N\}$  and the edge set  $\mathcal{E}_t$  containing available links. The graph matrix  $\mathbf{S}_t$  is the adjacency matrix with entry  $[\mathbf{S}_t]_{ij} = 1$  if  $(n_i, n_j) \in \mathcal{E}_t$  and  $[\mathbf{S}_t]_{ij} = 0$  otherwise. Additionally, we assume robot communications occur within the sampling time interval, such that robot action clock and communication clock coincide.

We use the WD-GNN to learn a decentralized controller  $\mathbf{U}_t = \Psi(\mathbf{X}_t; \mathbf{S}_t, \mathcal{A}, \mathcal{B})$  where the graph matrix  $\mathbf{S}_t$  is the adjacency matrix of the communication graph  $\mathcal{G}_t$  and the graph signal  $\mathbf{X}_t = [\mathbf{x}_{1,t}, \dots, \mathbf{x}_{N,t}]^\top \in \mathbb{R}^{N \times 6}$  is

$$\mathbf{x}_{i,t} = \left[ \sum_{j:n_j \in \mathcal{N}_{i,t}} (\mathbf{v}_{i,t} - \mathbf{v}_{j,t}), \sum_{j:n_j \in \mathcal{N}_{i,t}} \frac{\mathbf{p}_{i,t} - \mathbf{p}_{j,t}}{\|\mathbf{p}_{i,t} - \mathbf{p}_{j,t}\|^4}, \sum_{j:n_j \in \mathcal{N}_{i,t}} \frac{\mathbf{p}_{i,t} - \mathbf{p}_{j,t}}{\|\mathbf{p}_{i,t} - \mathbf{p}_{j,t}\|^2} \right], \quad \forall i = 1, \dots, N. \quad (36)$$

which collects position and velocity information of neighboring robots. Graph filters here are adapted to the delayed information structure as

$$\mathbf{B}(\mathbf{X}_t; \mathbf{S}_t, \mathcal{B}) = \sum_{k=0}^K \mathbf{S}_t \mathbf{S}_{t-1} \cdots \mathbf{S}_{t-k} \mathbf{X}_{t-k} \mathbf{B}_k. \quad (37)$$

We leverage the imitation learning to parametrize the optimal controller (34) with the WD-GNN.

**Dataset.** The dataset contains 400 trajectories for training, 40 for validation and 20 for testing. For each trajectory,  $N = 50$  robots are distributed randomly in a circle. The minimal initial distance between robots is 0.1m and initial velocities are sampled randomly from  $[-v, +v]^2$  with  $v = 3\text{m/s}$  by default. The duration of trajectories is  $T = 2\text{s}$  with the sampling time  $T_s = 0.01\text{s}$ ; the maximal acceleration is  $\pm 10\text{m/s}^2$  and the communication radius is  $r = 2\text{m}$ .

**Parametrizations.** For the WD-GNN, we consider the wide component as a graph filter and the deep component as a single layer GNN, where both have  $G = 32$  output features. All filters are of order  $K = 3$  and the nonlinearity is the Tanh. The output features are fed into a local readout layer at each node to generate two-dimensional acceleration  $\mathbf{u}_{i,t}$ . We train the WD-GNN for 30 epochs with batch size of 20 trajectories. The ADAM optimizer is used with decaying factors  $\beta_1 = 0.9$ ,  $\beta_2 = 0.999$  and learning rate  $\gamma = 5 \cdot 10^{-4}$ . We average experiment results for 5 dataset realizations.

**Performance measure.** The flocking condition can be quantified by the variance of robot velocities over network, referred as the *velocity variation*. At testing time, we measure the performance of

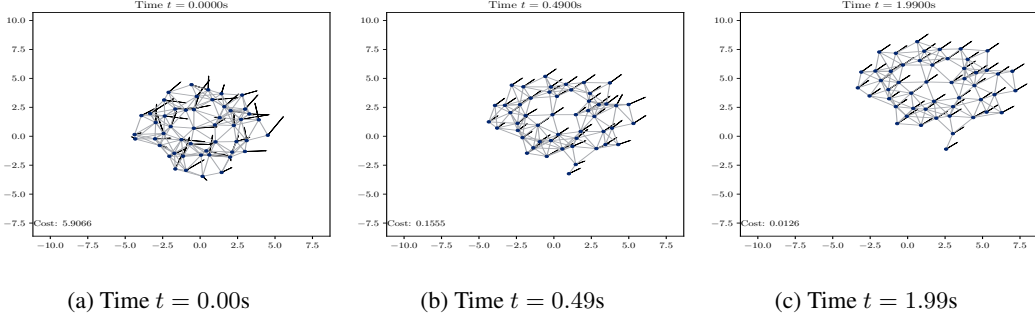


Figure 2. Video snapshots of the robot swarm flocking process with the learned WD-GNN controller.

learned controller from two aspects: the total velocity variation over the whole trajectory and the final velocity variation

$$\mathcal{J} = \frac{1}{N} \sum_{t=1}^D \sum_{i=1}^N \left\| \mathbf{v}_{i,t} - \frac{1}{N} \sum_{i=1}^N \mathbf{v}_{i,t} \right\|^2, \quad J(D) = \frac{1}{N} \sum_{i=1}^N \left\| \mathbf{v}_{i,D} - \frac{1}{N} \sum_{i=1}^N \mathbf{v}_{i,D} \right\|^2 \quad (38)$$

where  $D = T/T_s$  is the total number of time instances. The former reflects the whole controlling process which decreases if robots approach the consensus more quickly, while the latter indicates the final flocking condition of robots.

Main results are shown in the full paper. To further help understand and visualize this experiment, we show video snapshots of the robot swarm flocking process with the learned WD-GNN controller in Fig. 2. We see that robots move at random velocities initially in Fig. 2a, tend to move together in Fig. 2b, and are well coordinated in Fig. 2c. The cost shown in the figure is the instantaneous velocity variation of robots over network.

## C Experiment on movie recommendation systems

We consider another experiment on movie recommendation systems to corroborate our model. The goal is to predicate the rating a user would give to a specific movie [33]. We build the underlying graph as the movie similarity network, where nodes are movies and edge weights are similarity strength between movies. The graph signal contains the ratings of movies given by a user, with missing values if those movies are not rated. We train the WD-GNN to predict the rating of a movie of our choice, based on ratings given to other movies.

### C.1 Implementation details

We use a subset of MovieLens 100k dataset, which includes 943 users and 400 movies with largest number of ratings [34]. We compute the movie similarity as the Pearson correlation and keep ten edges with highest similarity for each node (movie) [33]. Each user is a graph signal, where the signal value on each node is the user rating given to the associated movie, with zero value if that movie is not rated. The dataset is split into 90% for training and 10% for testing. The rating of the movie of our choice is extracted as a label, and zeroed out in the graph signal.

We consider a WD-GNN comprising a graph filter and a single layer GNN. Both components have  $G = 64$  output features. All filters are of order  $K = 5$  and the nonlinearity is the ReLU. A local readout layer follows to map 64 output features to a single scalar predicted rating. We train the WD-GNN for 30 epochs with batch size of 5 samples, and use the ADAM optimizer with decaying factors  $\beta_1 = 0.9$ ,  $\beta_2 = 0.999$  and learning rate  $\gamma = 5 \cdot 10^{-3}$ . The performance is measured with the root mean squared error (RMSE) and the results are averaged for 10 random dataset split.

### C.2 Results

We first consider the WD-GNN without online retraining and compare it with the GNN and the graph filter (Table 2). We predict ratings for the movie *Star War* that has the largest number of ratings.

Table 2: Average (std. deviation) of the root mean squared error.

Architecture/Experiments	Train & test on same movie	Train on one & test on another
WD-GNN	0.8535( $\pm 0.0883$ )	1.0920( $\pm 0.1053$ )
Online WD-GNN (1 update)	0.8524( $\pm 0.1007$ )	0.9759( $\pm 0.0927$ )
Online WD-GNN (2 updates)	0.8442( $\pm 0.0993$ )	0.9815( $\pm 0.0902$ )
Online WD-GNN (3 updates)	0.8585( $\pm 0.1063$ )	0.9909( $\pm 0.0901$ )
GNN	0.8630( $\pm 0.0884$ )	1.0889( $\pm 0.1106$ )
Graph filter	0.8589( $\pm 0.0895$ )	1.0950( $\pm 0.1129$ )

We see that three architectures exhibit similar performance, while the WD-GNN performs best with the lowest RMSE. We also attribute this behavior to the increased learning ability of the WD-GNN obtained from its combined architecture. The second experiment considers the transferability, where we train the architectures on one movie (*Star War*) and use learned models to predict ratings for another movie (*Contact*). In this case, the problem scenario changes that creates a mismatch between the training and the testing, and all architectures suffer performance degradations. The GNN is slightly better, while followed closely by the WD-GNN and the graph filter.

We then run the WD-GNN with online learning. At testing time, we consider the system gets feedback from the user after predicting the rating, which is used as the instantaneous label for online learning. While the centralized online learning is available for recommendation systems, we keep in mind that the proposed WD-GNN can be retrained online in a distributed manner. We consider an online procedure with 400 testing users and for each user, the system performs the parameter update for 1, 2 and 3 times based on the instantaneous signal and feedback label, respectively. Results are shown in Table 2. We observe significant performance improvements when training and testing on different movies. In this case, the testing scenario differs from the one used for training, such that online learning adapts the WD-GNN to the new scenario and improves the transferability. We remark that these improvements will be emphasized as the testing phase further goes on. On the other hand, when training and testing on the same movie, online learning exhibits little effect (slight improvement) on the performance. This is because the problem scenario does not change much and the offline phase has already trained the WD-GNN well.

## D Online Wide and Deep GNN evaluation

Fig. 3 details the graph filter (graph convolution) [(3) in full paper] of order  $K = 3$  with  $F = 1$  input feature and  $G = 1$  output feature

$$\mathbf{B}(\mathbf{X}; \mathbf{S}, \mathcal{B}) = \sum_{k=0}^K b_k^{11} \mathbf{S}^k \mathbf{X}. \quad (39)$$

with filter parameters  $\mathcal{B} = \{b_0^{11}, \dots, b_K^{11}\}$ . In particular, the linear operator  $\mathbf{S}\mathbf{X}$ , also referred as graph shift operator, leverages the graph structure to process the graph signal. It assigns to each node the aggregated signal from immediate neighbors and collects the graph neighborhood information. Shifting  $\mathbf{X}$  for  $k$  times aggregates information from  $k$ -hop neighborhood yielding the  $k$ -shifted signal  $\mathbf{S}^k \mathbf{X}$ . With a set of parameters  $[b_0^{11}, \dots, b_K^{11}]^\top \in \mathbb{R}^{K+1}$ , the graph filter generates the higher-level feature that accounts for shifted signals up to a neighborhood of radius  $K$ , and thus reflects a more complete picture of network. As the shift-and-sum operation of graph signal  $\mathbf{X}$  over graph structure  $\mathbf{S}$ , the graph filter is also considered as the convolution in graph domain. If further particularizing  $\mathbf{S}$  the line graph and  $\mathbf{x}$  the signal sampled at time instances, the graph filter (39) reduces to the conventional convolution.

Algorithm 1 summarizes the proposed online learning algorithm for the WD-GNN.

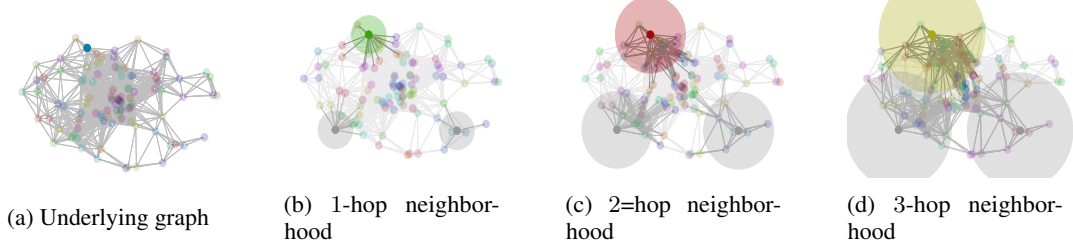


Figure 3. Graph filters perform successive local node exchanges with neighbors, where the  $k$ -shifted signal  $\mathbf{S}^k \mathbf{X}$  collects the information from  $k$ -hop neighborhood (shown by the increasing disks), and aggregate these shifted signals  $\mathbf{X}, \dots, \mathbf{S}^K \mathbf{X}$  with a set of parameters  $[b_0^{11}, \dots, b_K^{11}]^\top$  to generate the higher-level feature that accounts for the graph structure up to a neighborhood of radius  $K$ .

---

**Algorithm 1** Online Learning Algorithm for the WD-GNN

---

- 1: **Input:** offline learned parameters  $\mathcal{A}^\dagger, \mathcal{B}^\dagger$  by minimizing the ERM problem [(5) in full paper] over training dataset, and online step size  $\gamma_t$
  - 2: Fix the deep part parameters  $\mathcal{A} = \mathcal{A}^\dagger$  and set the initial wide part parameters  $\mathcal{B}_0 = \mathcal{B}^\dagger$
  - 3: **for**  $t = 0, 1, 2, \dots$  **do**
  - 4:   Observe instantaneous graph signal  $\mathbf{X}_t$ , graph matrix  $\mathbf{S}_t$  and loss function  $J_t(\cdot)$
  - 5:   Compute the instantaneous loss  $J_t(\Psi(\mathbf{X}_t; \mathbf{S}_t, \mathcal{A}^\dagger, \mathcal{B}_t))$
  - 6:   **if** requiring decentralized implementation **then**
  - 7:     Update the wide part parameters in a distributed manner
  - 8:     **for**  $i = 1, \dots, N$  **do**
  - 9:       
$$\mathcal{B}_{i,t+1} = \frac{1}{N_i+1} \left( \sum_{j:n_j \in \mathcal{N}_i} \mathcal{B}_{j,t} + \mathcal{B}_{i,t} \right) - \gamma_t \nabla_{\mathcal{B}} J_{i,t}(\Psi(\mathbf{X}_t; \mathbf{S}_t, \mathcal{A}^\dagger, \mathcal{B}_{i,t}))$$
  - 10:     **end for**
  - 11:   **else**
  - 12:     Update the wide part parameters in a centralized manner
  - 13:     
$$\mathcal{B}_{t+1} = \mathcal{B}_t - \gamma_t \nabla_{\mathcal{B}} J_t(\Psi(\mathbf{X}_t; \mathbf{S}_t, \mathcal{A}^\dagger, \mathcal{B}_t))$$
  - 14:   **end if**
  - 15: **end for**
-